Egypt. J. Chem. **Vol. 66**, No. 7 pp. 209 - 223 (2023)

Egyptian Journal of Chemistry

http://ejchem.journals.ekb.eg/

Antiviral and Antibacterial Properties of Synthesis Silver Nanoparticles with Nigella Arvensis Aqueous Extract

Mohamed E. Elnosary[1], Hesham A. Aboelmagd[2], Mahmoud R. Sofy[1*], Ahmed R. Sofy[1] and Ezzat H. Elshazly[2]**

[1] *Department of Botany and Microbiology, Faculty of Science, Al-Azhar University, 11884 Nasr City, Cairo, Egypt*

[2] *Department of Botany and Microbiology, Faculty of Science, Al-Azhar University, Assiut 71524, Egypt*

**The corresponded author: *Mahmoud R Sofy: Mahmoud_sofy@azhar.edu.eg*

*** Ezzat H Elshazly: ezzathamdy83@azhar.edu.eg*

Abstract

As a result of the emergence of new virus strains and the emergence of microorganisms resistant to various antibiotic synthetics, virus infections pose significant global health challenges, so the need for new therapeutic drugs rises as new viral and bacterial infectious diseases emerge. This study aimed to synthesize silver nanoparticles from Nigella arvensis aqueous extract and investigate their possible antiviral and antibacterial properties. X-ray diffraction, transmission electron microscopy, and UV-Visible spectroscopy were used to validate the synthesis of Ag-NPs. The findings are based on detecting Ag-NPs production through the shift from yellow color to dark brown color. TEM examination of Ag-NPs revealed spherical nanoparticles with mean sizes ranging from 2 to 9 nm and an average particle diameter of 2.5 nm. A UV-Visible spectrophotometric investigation revealed an absorption peak at λ max of 424 nm. However, Ag-NPs exhibit antimicrobial action against the four studied bacteria, with the inhibition zones for Bacillus subtilis ranging from 6 to 25 mm, Staphylococcus aureus from 8 to 25 mm, and Escherichia coli from 10 to 19 mm, whereas Pseudomonas aeruginosa has shown resistance to the AgNPs solution. The MBC varied from 22.3 to 36.8 µg/mL, whereas the MIC for the produced silver nanoparticles against the chosen bacterial strains ranged from 5.7 to 10.2 µg/mL. According to the maximum non-toxic concentration (MNTC) of Ag-NPs, 10.56 µg/mL, the greenly generated Ag-NPs of Nigella arvensis showed outstanding antiviral efficacy against HSV-1, HAV, and adenovirus by inhibiting replication by 53.6, 86, and 17.3 correspondingly. Finally, The novelty in this study is the application of silver nanoparticles as an antiviral against HSV-1, HAV, and adenovirus because of the high mutation of viruses.

Keywords: Ag-NPs, HSV, HAV, Adenovirus, MTT assay, cytotoxicity. Antimicrobial, Gram-positive, Gram-negative bacteria.

1. Introduction

Nanotechnology, which took two decades to develop, piqued the curiosity of scientists everywhere [1]. Nanoparticles have been produced using whole plants, microorganisms, plant tissue and fruits, marine algae, and plant extracts [2-4]. The plant extract Nigella arvensis has been used widely as a reducing and capping agent for the synthesis of AgNPs because it contains various phytochemicals compounds such as phenols, flavonoids, and terpenoids. Also, plant enzymes like hydrogenases, reductases, and quinones act as reductants in metal salts [5-7]. The green plant-mediated production of silver nanoparticles has grown in popularity owing to its ease of use, low cost, and environmental friendliness. In addition, it is safe to handle and has diverse metabolites, including antioxidant and antibacterial properties [8-10]. Because green nanoparticle synthesis happens extracellularly, metal production of nanoparticles using plant extract has an advantage over microbial-mediated biosynthesis. Furthermore, plant extracts have the potential to

*Corresponding author e-mail: * Mahmoud_sofy@azhar.edu.eg;** ezzathamdy83@azhar.edu.eg
EJCHEM use only: Received date 01 September 2022; revised date 22 September 2022; accepted date 03 October 2022
DOI: 10.21608/EJCHEM.2022.159976.6894

function as both reducing and stabilizing agents in the creation of nanoparticles [11, 12]. Moreover, this method is quick and suitable for large-scale production [13]. Scientists' emphasis on nanoparticles for their potent antiviral and antibacterial properties has increased due to the rising rates of antibiotic resistance [14, 15].

One of the most widely used examples of noble nanoparticles is silver nanoparticles (Ag-NPs), which are used for therapeutic purposes such as bio-labeling, tumor imaging, bio-sensing, and drug administration, as well as for food packaging, water filtering, cosmetics, and other uses [16-18]. Numerous studies have shown that Ag-NPs are a powerful biocidal agent against a variety of Gram-positive and Gram-negative bacteria, including multidrug-resistant bacteria and fungus pathogens [19, 20]. In addition, there has been evidence of activity of Ag-NPs against Pseudomonas aeruginosa and Vibrio cholera, methicillin-resistant Staphylococcus aureus (MRSA) [21], Escherichia coli [22]. The growth of P. aeruginosa and E. coli was consistently inhibited by low amounts of Ag-NPs [23-25]. Silver nanoparticles showed synergistic antimicrobial activity against Salmonella typhi, S. aureus, E. coli, and Micrococcus luteus when combined with penicillin, amoxicillin, ampicillin, clindamycin, kanamycin, chloramphenicol, erythromycin, and vancomycin [26]. One of the effective mechanisms by which Ag-NPs affect bacteria is interacting with proteins in thiol (-SH) groups, where it binds to the bacterial cell wall and cell membrane. Damage observed in membranes that come into contact with Ag-NPs causes leakage of cellular contents and, thus, cell death. Nanoparticles with a smaller diameter have a larger surface area, and it has been observed that these particles have more antibacterial activity [27-30]. One of the main causes of illness and mortality globally is viruses. Viral diseases have a huge impact on the economy around the world as they cause diseases such as various herpes virus problems (shingles, chickenpox, infectious mononucleosis, genital herpes, viral encephalitis or herpes keratitis) and hepatitis viruses [31]. About 50% to 90% of people worldwide have HSV-1 infection, making it one of the most widespread viruses. Approximately 90% of people have HSV-1 seroprevalence [32]. Currently, the most often used anti-HSV medications in clinical practice are nucleoside analogs as penciclovir, famciclovir, acyclovir (ACV), and others. Acyclovir is regarded as the gold standard for the treatment of HSV-1 infection [33]. ACV can specifically inhibit the virus' DNA polymerase to stop its replication and eventually stop the generation of HSV-1 offspring by being phosphorylated by viral thymidine kinase and cellular kinase [34, 35]. However, mounting evidence is that overuse of nucleoside analogs, such as ACV, might promote the formation of HSV-1 mutants resistant to treatment [36]. It has been discovered that the HSV-1 genome's mutations, insertions, or deletions might result in viral resistance, which was very unfriendly to conventional antiviral medications [37]. Therefore, a significant barrier to effectively curing HSV-1 infection has been established by the proliferation of prevalent drug-resistant HSV-1 strains [38]. Additionally, some studies indicate that prolonged use of ACV may have some adverse effects, including skin rashes, nerve poisoning, nausea, vomiting, stomach discomfort, and diarrhea [39]. Research and development of novel and effective anti-HSV-1 medications are urgently needed due to the increasing resistance of HSV-1 to conventional medications and the present lack of availability of the HSV vaccine for the worldwide market.

So many studies have used green nanotechnology to take advantage of both cutting-edge and useful nanoscale materials. In recent years, its ongoing development has created exceptional chances for creating nanoparticle drugs that are effective against viruses. Adenovirus, Hepatitis B virus, and Herpes simplex virus types I and II (HSV-I and HSV-II) are a few examples of the various human pathogenic viruses that Ag-NPs have a potent antiviral impact against (HBV) [40].

In this study, the safe, therapeutic, and cytotoxic concentrations of Ag-NPs were synthesized by the green nanotechnology method for determined in vitro with an emphasis on the inhibitory effect of Ag-NPs on Gram-positive (Bacillus subtilis ATCC 6633, Staphylococcus aureus ATCC 7984) and Gram-negative (Escherichia coli ATCC 8739, Pseudomonas aeruginosa ATCC 9027,) bacterial and viral replication (HAV, HSV-1, and adenoviruses as a model). The novelty in this study is the application of silver nanoparticles as antiviral against HSV-1, HAV, and adenovirus due to the high mutation of viruses.

2. Material and methods

Plant material

In January 2022, the Agriculture Research Center in Giza, Egypt, supplied the Nigella sativa seeds with aqueous extract. First, deionized water was used to wash the Nigella sativa seeds in aqueous extract. Next, the seeds were shade dried at room temperature for 24 hours to remove moisture. Finally, a clean electric blender was used to pulverize the seeds to obtain a fine powder, which was then stored in an amber glass bottle to prevent light exposure.

Chemicals and Reagents

This study used silver nitrate ($AgNO_3$) purchased from Sigma-Aldrich, Germany, with a 99.5% purity.

Preparation of seed extract

Twenty grams of coarsely powdered Nigella sativa seeds aqueous extractwere cooked in 100 milliliters of two-fold distilled water for three minutes before being filtered by Whatman No 1 filter paper. The filtrate was stored and collected at 4 °C for later use.

Green synthesis of Ag-NPs

One mM AgNO3 and aqueous Nigella sativa seeds aqueous extractwere used to make Ag-NPs. 4 mL aqueous seed extractwas added to 96 mL AgNO3 exposed to sunshine. The solution's color change was monitored regularly. As a result, the aqueous seed extractchanged from yellow to dark brown color, indicating that Ag-NPs were made from the seeds[6].

Characterization of Ag-NPs by Ultraviolet-visible (UV-visible) analysis

In order to display the full biological reduction of $AgNO_3$ to Ag-NPs, 1 mL of the sample suspension was diluted with two mL of distilled water. Also, a UV-visible spectrophotometer (Shimadzu UV probe 1800) was used to record the spectrum of the sample within a scan range of 200 to 700 nm.

Characterization of Ag-NPs by X-ray diffraction (XRD) analysis

Analytical XRD was applied in the present study with a scanning rate of 20 min1, a monochromatic filter in the 2 range of 10-80, and an operating voltage of 40 kV. It was utilized to investigate phase identification and crystal structure characterization of nanoparticles.

Characterization of Ag-NPs by Transmission Electron Microscopy (TEM) analysis

The size and morphology of the fabricated Ag-NPs are examined using TEM. The work was conducted using a 200 kV ultra-high-resolution TEM (JEOL, JEM 2100 h with EELS). The TEM grid was created by spotting five µL of Ag-NPs solution onto a carbon-coated copper grid and drying it under a lamp[6].

Characterization of Ag-NPs by FTIR analysis

Fourier transform infrared spectroscopy FTIR spectra were used to examine the FTIR spectra N. sativa seedaqueous extractAgNPs samples. The FTIR analysis was carried out with KBr pellets and recorded in the 400-4,000 cm-1 range. The various vibration modes were recognized and allocated to determine the different functional groups in the samples.

Antiviral activity

Utilizing the MTT test, antiviral activity was assessed[41].

VERO cells and viruses

All viruses came from the microbiology department of the Faculty of Medicine at Al-Azhar University in Cairo, Egypt. VERO cells (ATCC: CCL-81) were acquired from Vacsera Research Foundation, Egypt.

Determination of Ag-NPs cytotoxicity on VERO cells

The maximum non-toxic concentration (MNTC) of every Ag-NPs was evaluated by two-fold dilutions in MEM with FCS, beginning with 169 ug/ml and continuing to a 10^{-6} dilution.

A series of Ag-NP concentrations were prepared, and the growth medium from 96-well microtiter plates was decanted. VERO cells were twice washed with wash media, and double-fold dilutions of the tested sample were made in minimum essential media once the monolayer had formed. Incubation was conducted with 0.1 mL of each dilution in different wells, leaving three wells as controls. The physical characteristics of toxicity, such as partial or total loss of the monolayer, cell granulation, shrinkage, or rounding, were examined in the cells.

5 mg/mL of PBS was used to make the MTT solution (BIO BASIC CANADA INC). Each well received 20 µL of the MTT solution, which was then

thoroughly mixed with the medium by placing each well on a shaking table for five minutes at 150 rpm. The MTT was metabolized at (37 °C, 5% CO_2) for 1–5 hrs, after which the medium was removed (if necessary, dry the plate on paper towels). Additionally, formazan is re-suspended in 200 µL of DMSO and shaken at 150 rpm for five minutes to properly combine the formazan and solvent. At 560 nm, the optical density is calculated, and at 620 nm, the background is removed. Optical density and cell count ought to be closely connected. Each extract's maximum non-toxic concentration (MNTC) was established and utilized for further biological research [41, 42].

MTT assay protocol

A 96-well plate with 10,000 cells plated in 200 µL of medium per well was used to measure the antiviral activity. After incubating the virus suspension and equal volumes (1:1 v/v) of the tested sample for one hour, 100 µL of the viral/sample suspension is added. The mixture is shaken at 150 rpm for 5 minutes. The three wells for blank controls are left empty. The remaining wells are incubated at (5 percent CO_2, 37 °C) to allow the cells to attach to the wells overnight. To give the virus time to work, the viral/sample suspension is incubated at (5% CO_2, 37°C) for one day. Next, 20 mL of MTT solution is added to each well of 96-well plates, which should have at least 2 mL of MTT solution per well. The MTT solution should be completely mixed with the medium by shaking the plates at 150 rpm for 5 minutes. The plate is then incubated for 1–5 hours at (37°C, 5 percent CO_2) to enable the MTT to be digested, after which the media is removed (dry plate on paper towels to remove residue if necessary). Next, Formazan (MTT metabolic product) is re-suspended in 200 µL DMSO and shaken at 150 rpm for five minutes to mix the two substances completely. At 560 nm, the optical density is calculated at 620 nm, and the background is removed. There should be a direct relationship between optical density and cell number [41, 42]. The findings of the 50% cytotoxic concentrations (CC50) and 50% inhibitory concentrations (IC_{50}) were calculated using the GraphPad PRISM program (Graph-Pad Software, San Diego, USA).

Antibacterial activity

Four bacterial strains (Bacillus subtilis ATCC 6633, Staphylococcus aureus ATCC7984, Escherichia coli ATCC 8739, and Pseudomonas aeruginosa ATCC 9027) were obtained from the American Type Culture Collection by Sigma-Aldrich (import company) were used in this study.

Determination of Ag-NPs antibacterial activity assay using well diffusion method (WDM)

The agar well diffusion method by Mueller Hinton agar (MHA) (Oxoid, UK) (2.0 g/L beef infusion solids, 17.5 g/L casein hydrolysate, and 1.5 g/L starch in 1000 mL distilled water, at pH 7.4 ± 0.2) was used to evaluate the antibacterial activity of Ag-NPs stock solution (170 µg/mL). A sterile spreader inoculated the agar surface by spreading a bacterial suspension containing approximately 1.5 X 107 CFU/mL over the entire surface. A hole with a diameter of 6 mm has punched aseptically with a sterile cork borer, and then the Ag-NPs solutions (100 µL) were added to the well using a micropipette. Three wells are made for saline (0.85%) solution as a negative control, chloramphenicol as a positive control, and Ag-NPs stock solution in the first plate. In the second plate, five different concentrations of the Ag-NPs stock solution were investigated, containing 170, 85, 42.5, 21.3, and 10.6µg/mL. Agar plates were incubated for 24 h at 37 °C, and zones of inhibition for all plates were determined. To determinethe MIC of Ag-NPs, the standard broth dilution method (Clinical and Laboratory Standards Institute, CLSI M07-A9) was used to evaluate the visible growth of microorganisms in the Mueller Hinton broth (MHB) medium. Firstly, serial two-fold dilutions of Ag-NPs in concentrations ranging from 170 to 10.6 µg/ml in a liquid growth medium were distributed in tubes containing about 2 mL (macrodilution). Then, each tube is inoculated with a microbial inoculum adjusted to (108 CFU/ml, 0.5 McFarland's standard), and the microbial suspension was prepared in the same medium. One tube is considered the control tube, which contained only inoculated broth and was incubated for 24 h at 37 ^{O}C. The minimum inhibitory concentration (MIC) endpoint is the lowest concentration of the tested specimens, where no visible growth is seen in the tubes[43]. The minimum bactericidal concentration (MBC) can be determined after broth macro dilution by sub-culturing samples from tubes that gave a negative microbial growth on the surface of plates with MHA medium. To determine the number of viable cells (CFU/mL) after

incubation for 24 h under a standardized set of inoculation and incubation described in document M26-A. The bactericidal endpoint (MBC) is defined as the lowest concentration; at which 99.9% of the final bacterial inoculum is killed.

Data analysis

The antiviral and antibacterial activity of Ag-NPs were analyzed using Minitab 19. A P-value < 0.05 was considered significant. Tukey test for pairwise and one-way ANOVA comparisons was used for post hoc analysis of all group interactions. Post-hoc analysis results are shown as letters, with groups that share the same letter being non-significantly different and distinct letters expressing significant differences across various groups.Values are presented as the mean±SD of the three replicates of each experiment.

Results

Synthesis and characterization of Ag-NPs

The color of the reaction media progressively changed from yellow to dark brown, indicating the success of the green production of silver nanoparticles utilizing Nigella Sativa Seeds aqueous extract (Fig. 1).

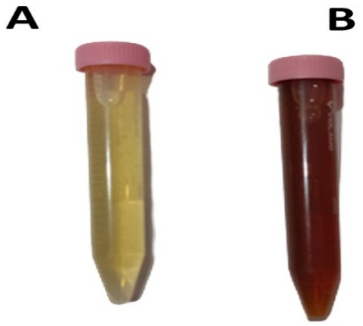

Fig. 1. Change the color of the solution from A) yellow to B) dark brown.

UV- visible spectroscopy characterization of the synthesized Ag-NPs

UV- visible spectroscopyindicated that the silver nitrate in aqueous solution was reduced to surface plasmon vibrations in silver nanoparticles. Furthermore, the UV-vis spectrum analysis of biosynthetic Ag-NPs revealed a peak at 424 nm (Fig. 2) within the specified range of Ag-NPs. It indicated their presence in the reaction mixture.

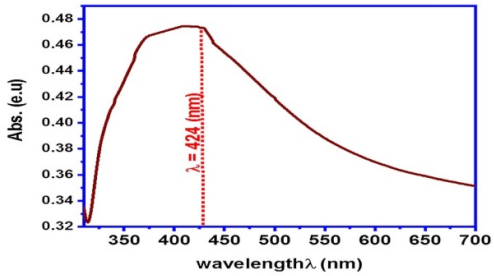

Fig. 2 UV-Vis spectrum of biosynthesized Ag-Nps

XRD characterization of the synthesized Ag-NPs

The XRD examination revealed four different diffraction peaks at 38, 45, 64, and 77, which may be related to the angles of the spherical Ag crystals at 111, 200, 220, and 312. This research showed that orthorhombic crystals make up nanoparticles. Furthermore, the analysis's high peaks show an active silver composition with indexing (Fig. 3). As a result, the XRD verifies that the silver nanoparticles have crystallized, and it is evident that the compound's angle value is stable.

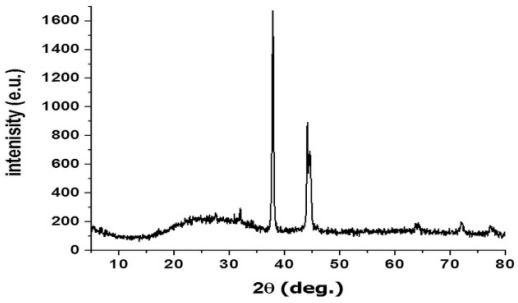

Fig. 3 XRD of silver nanoparticles from N. sativa, the calculated average particle size of AgNPs sample is 7.48 nm.

TEM characterization of the synthesized Ag-NPs

Nanoparticles' composition and size distribution might be seen using a transmission electron microscope. The TEM and particle size distribution images of Ag-NPs obtained in this investigation are

presented in Figs.(4 A & B), with particle sizes ranging from 2–9 nm and an average particle diameter of 2.5 nm determined using published methods and a standard deviation of 0.73. This data was in good agreement with the XRD analysis result, which confirmed the formation of NPs. Furthermore, the Ag-NPs were found to have spherical forms with a narrow size distribution.

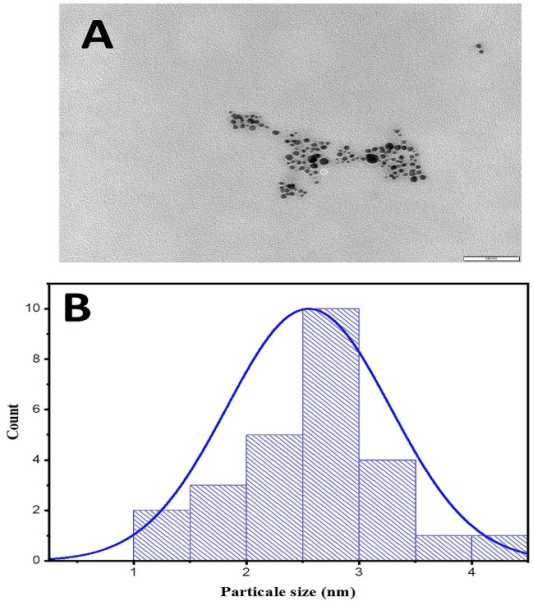

Fig. 4 TEM photos for (A) shape and (B) size of produced Ag-NPs of Nigella Sativa

FTIR characterization of the synthesized Ag-NPs

Absorption bands at 3345 cm^{-1} (O-H stretching, H-bonded of alcohols and phenols, and N-H stretching of primary and secondary amines of plant protein), 2924 and 2849 cm^{-1} (C-H stretching), 1627 cm^{-1} (-C=C stretching and N-H bend), 1440 cm-1 (C-C stretching), and 1034 cm^{-1} (C-O stretching of alcohols, carboxylic acids, esters, and ether were discovered. After bioreduction, both experiments showed a shift in the absorption bands from 3345 to 3360, 2924 to 2915, 1627 to 1637, and 1440 to 1010 cm^{-1}, indicating that the vibrational bands that correspond to bonds like -C=C and -C=O are caused by compounds like flavonoids and alkaloids in N. sativa seeds (Fig 5).

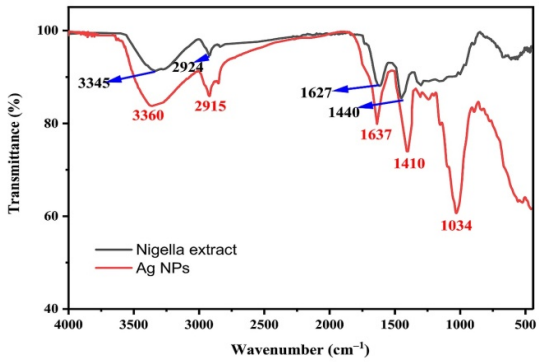

Fig. 5 FTIR analysis Ag-NPs of Nigella Sativa

Antiviral Activity

Ag-NPs was evaluated by two-fold dilutions in MEM with FCS, by preparing six concentrations of it, beginning with 169 ug/mL followed by 84.5 ug/mL, 42.5 ug/mL, 21.13 ug/mL, 10.56 ug/mL and 5.28 ug/mL. The cytotoxicity of nanoparticles was evaluated on VERO cells using the MTT assay to ensure that the measured Ag-NPs doses were not harmful. The cytotoxicity concentration (CC50) of Ag-NPs is 36.3, (Figs.6& 7 a - g).

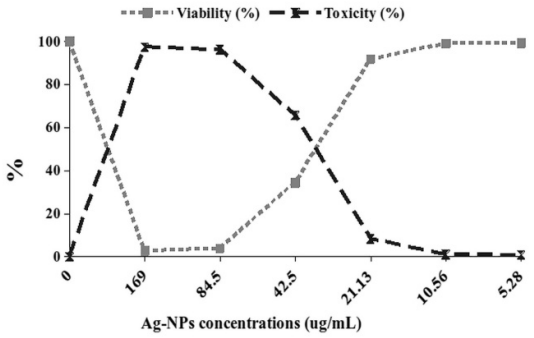

Fig. 6. Cell viability and cytotoxicity of Ag-NPs concentrations on Vero cell

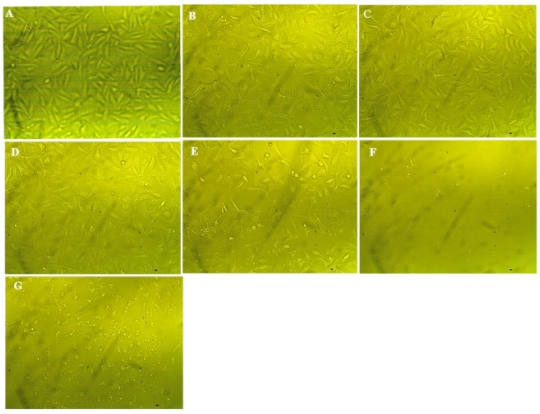

Fig. 7. Morphological changes of Vero cells treated with Ag-NPs at different concentrations (x 10 magnification). (A) Control Vero cell, (B) 5.28 ug/ml Ag-Nps, (C) 10.56 ug/ml Ag-Nps, (D) 121.13 ug/ml Ag-Nps, (E) 42.25 ug/ml Ag-Nps, (F) 84.5 ug/ml Ag-Nps, (G) 169 ug/ml Ag-Np

. The antiviral and cytotoxicity of the materials against HAV, HSV-1, and adenovirus viruses were investigated using the MTT antiviral test methodology. The results revealed that the different concentrations of Ag-NPs have activity against three viruses. The dose of 10.56 ug/mL of Ag-NPs was promising, inhibited replication of HAV with 86%, moderately inhibited replication of HSV-1 with 53.6%, and mildly inhibited replication of adenovirus with 17.3%. On the other hand, the dose of 5.28 ug/mL of Ag-NPs has mildly inhibited replication of HSV-1, HAV, and adenovirus with 31.53%, 37.99%, and 8.33%, respectively (Fig. 8).

On the other hand, the finding that Ag-NPs had a cytotoxic concentration (CC 50) of 52.17ug/mL and IC 50 of 6.45, 11.67, and 4.05 for HSV-1, HAV, and adenovirus, respectively,and a selective index (SI) of 12.1 (Table 1).

Table 1.
Antiviral activity of Ag-NPs against HSV-1, HAV, and adenovirus

Compound name	Virus name	CC50 (ug/ml)	IC50 (ug/ml)	SI
Ag-NPs	HSV-1	52.17	8.22	6.45
	HAV		4.47	11.67
	adenovirus		12.89	4.05

CC50:cytotoxic concentration, IC50: half maximal inhibitory concentration, SI: selective index

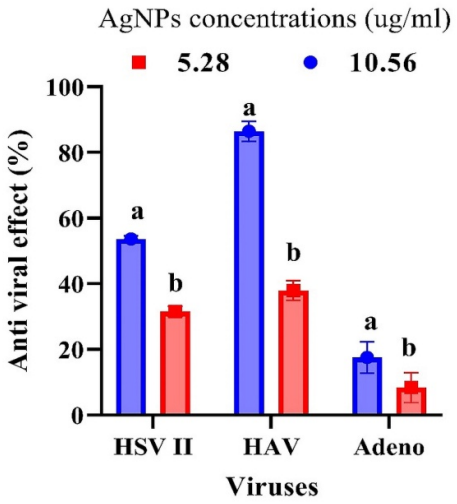

Fig. 8. The Vero cell line was used to study the antiviral activity of free silver nanoparticles (Ag-NPs) against the hepatitis A virus (HAV), the herpes simplex virus type 1 (HSV-1), and the adenovirus (Adeno). Ag-NPs' antiviral activity was quantified as a percentage compared to untreated (control) infected Vero cells in the MNTC range. Figures that show significance have a p-value < 0.05, and (a, b, c, and d letters mention significant when they are different and non-significant in similar).

Antibacterial activity

Evaluation of the antibacterial activity of Ag-NPs (In-vitro):

The antimicrobial activity using the well diffusion method against B. subtilis, S. aureus, E. coli, and P. aeruginosa is presented in Figs(9, 10) and Table (2).After a Twenty-four-hour incubation, Gram-positive strains (B. subtilis and S. aureus) showed good inhibition zone (IZ) for both tested samples and positive control. In contrast, in E. coli the tested sample had little effect compared to the positive control. The negative control has no effect on the tested isolates (Fig. 8).Based on the data obtained from the plates (MHA), the inhibition zone for B. subtilis ranged from 6 to 25 mm, S. aureus from 8 to 25 mm, E. coli from 10 to 19 mm. At the same time,P.aeruginosa showed resistance to Ag-NPssolution. For MIC and MBC determination, and according to the results acquired from the in vitro antimicrobial assays, the MIC for the synthesized silver nanoparticles (Ag-NPs) against the selected bacterial strains ranged from 5.7 to 10.2µg/mL. In contrast, MBC ranged from 22.3 to 36.8µg/mL, as shown in Table (3).

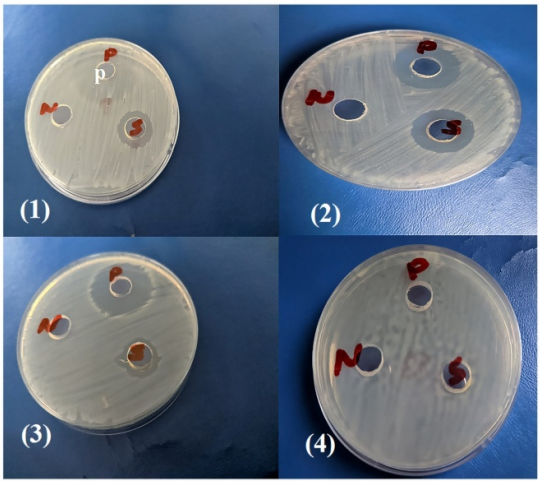

Fig. 9. Antimicrobial susceptibility well diffusion method. Zones of inhibition of positive control (P), negative control (N), and Ag-NPs (S) against the pathogenic strains B. subtilis (1), S.aureus (2), E. coli (3), and P. aeruginosa (4).

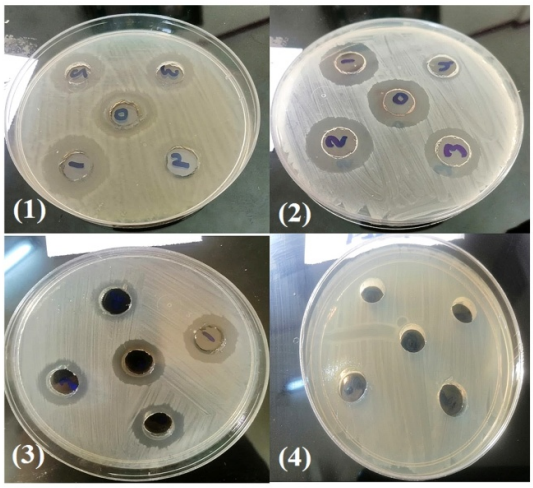

Fig. 10. Antimicrobial susceptibility well diffusion method. Zones of inhibition of silver nanoparticles against the pathogenic strains B. subtilis (1), S.aureus (2), E. coli (3), and P. aeruginosa (4)

Discussion

Recently, biological or green chemistrysynthesis of NPs received enormous attention over the physical and chemical synthesis, as it is environment-friendly solvents, biocompatible and non-toxic reagents. Microorganisms, whole plants, plant tissue and fruits, plant extracts, and marine algae have been used to produce nanoparticles[44]. However, plant extract mediated synthesis of metal nanoparticles has theedge over microbial mediated biosynthesis of nanoparticles because the green synthesis of nanoparticles takes place extracellular. In addition, plant extracts may act both as reducing agents and stabilizing agents in the synthesis of nanoparticles[45]. Further, this process is quick and suitable for large-scale synthesis[46].

The aqueous extracts of Nigella arvensis were used to create the Ag-NPs, and the reaction mixture's color shift proved that Ag-NPs had been produced. After incubation at room temperature, the emergence of a dark brown hue indicated the synthesis of Ag-NPs[47, 48]. In the UV-visible spectrum, Ag+ ions were shown to be reduced. Ag-NPs' size and shape might reflect the absorption peak. The peak intensity and the size of the nanoparticles are linearly correlated. The current study's findings support the creation of spherical nanoparticles with an average size range of 2–9 nm and an estimated average particle diameter of 2.5 nm calculated using TEM.

The probable biomolecules in N. sativa seed that may be responsible for reducing and capping the reduced silver nanoparticles were identified using FTIR analyses. In addition, their potential roles in the synthesis of silver nanoparticles were also predicted. To do this, the band intensities for the control and test materials (before and after the reaction with silver nitrate, respectively) were examined in various spectral areas, as shown in(Fig. 5) According to the findings, absorption bands at 3345 cm^{-1} (O-H stretching, H-bonded of alcohols and phenols, and N-H stretching of primary and secondary amines of plant protein), 2924 and 2849 cm^{-1} (C-H stretching), 1627 cm^{-1} (- C=C stretching and N-H bend), 1440 cm^{-1} (C-C stretching), and 1034 cm^{-1} (C-O stretching of alcohols, carboxylic acids, esters, and ether[49, 50]

After bioreduction, both experiments demonstrated a shift in the absorption bands from 3345 to 3360, 2924 to 2915, 1627 to 1637, and 1440 to 1010 cm^{-1}, indicating that the compounds like flavonoids and alkaloids in N. sativa seeds are what cause the vibrational bands that correspond to bonds like -C=C and -C=O. Inferring from this, it is believed that these biomolecules, along with a few proteins, are in charge of capping, stabilizing, and reducing Ag+ to Ag NPs[50]. The FTIR analysis revealed that the synthesized Ag NPs contained amides, alkanes, carboxyls, alcohols, and phenols

The current work describes the environmentally friendly production of Ag-NPs utilizing Nigella arvensis aqueous and their use in preventing the

spread of adenovirus, HAV, and HSV-1 infections. According to the data, the Nigella arvensis biosynthesized Ag-NPs improved the antiviral activity against the three tested viruses. Although the antiviral mode of action of green-produced Ag-NPs has not been identified, Ag-NPs' antiviral efficacy against some viruses is most likely owing to their ability to bind to viral envelope glycoproteins, inhibiting viral entry into the host cell[51, 52]. Additionally, Ag-NPs may enter the viral cell and exert their antiviral activity by interacting with the viral genome (DNA or RNA) or obstructing the pathways necessary for viral replication. It has also been reported that SNPs have antiviral activity against a variety of viruses, including the herpes simplex virus[53] and hepatitis virus[52].

Additionally, Ag-NPs may decrease viral replications in host cells by blocking viral attachment to or replication on host cells. However, it has been proposed that the antiviral action of silver nanoparticles is caused by two different processes that prevent viral replication: 1- Ag-NPs may interact with viral components and double-strand breaks when they traverse cell membranes[54, 55]. 2- Ag-NPs have the ability to attach to sulfur-containing residues on the surface glycoproteins of viruses, preventing viral-host penetration and cell binding, and leaving the virus in the extracellular space where it cannot spread.2- Ag-NPs have the ability to attach to sulfur-containing residues on the surface glycoproteins of viruses, preventing viral-host penetration and cell binding, and leaving the virus in the extracellular space where it cannot spread[56, 57].

Due to the emergence of resistance of microorganisms to various antibiotic synthetics, new antimicrobial agents have been developed to prevent infections caused by pathogenic microorganisms. So,one of the goals of this work was to determine the antibacterial effect of silver nanoparticles against four bacterial strains (S. aureus, B. subtilis,E. coli, and P. aeruginosa). The antimicrobial effects of silver are mostly attributed to silver ions[58, 59]. Silver nanoparticles provide a greater and better bactericidal action due to their larger surface area[60, 61]. Minimum inhibitory concentration values of Ag-NPs against the four bacterial strains showed differences from strain to other. The major reason supporting this difference in the sensitivity to Ag-NPs is the variation in cell wall composition between Gram-positive and negative bacteria[62]. Bacteria of both the gram-positive and gram-negative types are killed by silver nanoparticles[63-65]. Among the different concentrations tested, the Ag-NPs showed a lower MIC for E. coli where the MIC values were 10.2, 6.31, and 5.72 µg/mL for S. aureus, B. subtilis, and E. coli, respectively. The MIC recorded for B. subtilis in this study was lower than those reported inHuang, et al. [66] and lower than in other studies[67, 68]. Also, the MIC recorded for S. aureus results in this study were higher than those reported inGaribo, et al. [69] but in a lower concentration compared to other findings[67]. The lowest inhibitory concentration for E. coli was similar to that reported by Huang, et al. [66]. Still, it was higher than those found inGaribo, et al. [69] and lower than those found in other studies[70-72]. The preparation process and size of the silver nanoparticles utilized might be to blame for the variations in the effective concentrations of Ag-NPs across studies. At lesser doses, the ultrafine particle size induces its activity[73, 74]. Also, in this study, P. aeruginosa showed resistance to silver nanoparticles even at high concentrations. This resistance of P. aeruginosa to Ag-NPs was reported in several studies, as[75, 76] concluded that P. aeruginosa was able to develop resistance to silver nanoparticles, andHosny, et al. [77] plasmid-mediated silver resistance in clinical bacteria, such as P. aeruginosa isolates, has been discovered.

Previous studies indicated the antibacterial activity of AgNPs by attachment to the bacterial cell wall or the formation of free radicals[78, 79]. In addition, the silver ions released from AgNPs may play a vital role inantibacterial activity due to the interaction of silver ions with the thiol groups of enzymes [80]. Furthermore, it was shown that the antibacterial activity of AgNPs was size and shape-dependent. AgNPs (1–10 nm) attach to the surface of the cell membrane and drastically disturb its proper function, like respiration and permeability [81].

Conclusion

The green synthesis of silver Nanoparticles with Nigella arvensis Aqueous Extractwas verified by examining the reaction mixture's color change. UV-visible, RXD, and TEM characterized the produced Ag-NPs, and their diameters vary from 2 to 9 nm, with an average particle diameter of 2.5 nm. At the suggested dose of 10.56 g/mL, Ag-NPs may be utilized in vitro safely to shield the cellular culture

against viral replications. When given prior to viral infection, Ag-NPs could suppress HAV and HAS-1 at non-toxic quantities. Gram-negative and Gram-positive strains were used to evaluate the antimicrobial activity, and the findings indicated that both the qualitative diffusion in wells test and the quantitative MIC and MBC test significantly inhibited the growth of bacteria. The fact that P. aeruginosais resistant to silver nanoparticles is a significant research restriction. Further research is needed to evaluate the antibacterial impact of silver nanoparticles on various bacterial strains.

Table 2.
The diameter of the inhibition zone (mm) of AgNPs against the selected bacterial strains

Bacterial strains		Concentration (µg/mL)				
		170	85	42.5	21.3	10.6
B. subtilis	Inhibition zone (mm)	29±0.4 a	29±0.2 a	26±0.3 a	19±0.1 a	10±0.0 a
S. aureus		29±0.2 a	27±0.2 a	27±0.3 a	22±0.2 a	12±0.0 a
E. coli		23±0.2 b	23±0.1 b	21±0.2 b	21±0.2 a	14±0.0 a
P. aeruginosa		0.0±0 c	0.0±0 c	0.0±0 c	0.0±0 b	0.0±0 b

* Values in a column assigned with different letters denote significant difference ($p < 0.05$)

Table 3.
MIC and MBC (µg/mL) of Ag-NPs against the selected bacterial strains

Clinical bacterial strains	Concentration (µg/mL)	
	MIC	MBC
B. subtilis	10.2±0.41	36.8±0.76
S. aureus	6.31±0.22	24.5±0.67
E. coli	5.72±0.23	22.3±0.60

Bacillus subtilis (B. subtilis), Staphylococcus aureus (S. aureus), Escherichia coli (E. coli), Minimum inhibitory concentration (MIC), Minimum bactericidal concentration (MBC)

Abbreviations:

Abbreviation	Full name	Abbreviation	Full name
Ag-NPs	Silver nanoparticles	M. *luteus*	*Micrococcus luteus*
TEM	Transmission electron microscope	ACV	acyclovir
MNTC	Minimal non-toxic concentration	WDM	well diffusion method
HSV-1	Herpes 1 virus	MHA	Mueller Hinton agar
HAV	Hepatitis A virus	MBC	The minimum bactericidal concentration
S. aureus	*Salmonella typhi*	IC50	Inhibition concentration 50%
E. coli	*Escherichia coli*	SI	Selective index

Declarations

N/A

Ethics approval and consent to participate

Not applicable.

Consent for publication

Not applicable.

Availability of data and materials

Not available.

Competing interests

The authors declare no competing interests.

Funding

No funding source was provided.

Author's Contribution

Author contribution ME, HA, MR, AR, and EH performed the literature search, collected the data in tables, prepared the figures, and wrote the first draft. ME, HA and EH conceptualized the idea, and MR, AR and ME edited and proofread the manuscript before its submission. All authors have read and agreed to the final version of the manuscript.

References

[1] Singh, T., Shukla, S., Kumar, P., Wahla, V., Bajpai, V.K., Rather, I.A., Application of nanotechnology in food science: perception and overview, Frontiers in microbiology, 8, 1501 (2017).

[2] Maksoud, M.A., Bekhit, M., El-Sherif, D.M., Sofy, A.R., Sofy, M.R., Gamma radiation-induced synthesis of a novel chitosan/silver/Mn-Mg ferrite nanocomposite and its impact on cadmium accumulation and translocation in brassica plant growth, International Journal of Biological Macromolecules, 194, 306-316 (2022).

[3] Fouda, H.M., Sofy, M.R., Effect of biological synthesis of nanoparticles from Penicillium chrysogenum as well as traditional salt and chemical nanoparticles of zinc on canola plant oil productivity and metabolic activity, Egyptian Journal of Chemistry, 65, 1-2 (2022).

[4] Rehan, M., Nada, A.A., Khattab, T.A., Abdelwahed, N.A., Abou El-Kheir, A.A., Development of multifunctional polyacrylonitrile/silver nanocomposite films: Antimicrobial activity, catalytic activity, electrical conductivity, UV protection and SERS-active sensor, Journal of Materials Research and Technology, 9, 9380-9394 (2020).

[5] Khattab, T., Mashaly, H., Ahmed, H., Rehan, M., Multi-stimuli Responsive Natural Fibers Immobilized with Silver Nanoparticles via Plasma-activated Generation of Polyaniline, Egyptian Journal of Chemistry, 65, 1-2 (2022).

[6] Chahardoli, A., Karimi, N., Fattahi, A., Nigella arvensis leaf extract mediated green synthesis of silver nanoparticles: Their characteristic properties and biological efficacy, Advanced Powder Technology, 29, 202-210 (2018).

[7] Chahardoli, A., Karimi, N., Fattahi, A., Biosynthesis, characterization, antimicrobial and cytotoxic effects of silver nanoparticles using Nigella arvensis seed extract, Iranian journal of pharmaceutical research: IJPR, 16, 1167 (2017).

[8] AlMasoud, N., Alhaik, H., Almutairi, M., Houjak, A., Hazazi, K., Alhayek, F., Aljanoubi, S., Alkhaibari, A., Alghamdi, A., Soliman, D.A., Green nanotechnology synthesized silver nanoparticles: Characterization and testing its antibacterial activity, Green Processing and Synthesis, 10, 518-528 (2021).

[9] Hamouda, N.H., Youssef, H.F., Saleh, W.D., El Sabry, M.I., Nasr, N.F., Chemical and Green Silver Nanoparticles: Synthesizing, Characterizing, and Antimicrobial Activity Against Microorganisms in Hatchery Plants, Egyptian Journal of Chemistry, (2022).

[10] Nguyen, T.T.T., Le, H.H., Truong, T.V., Doan, T.P.T., Nguyen, T.T.T., Nguyen, T.M.L., Application of the Response Surface Methodology for Green synthesis of silver nanoparticles using a plant extract of shallot, Egyptian Journal of Chemistry, 63, 4579-4588 (2020).

[11] Mittal, A.K., Chisti, Y., Banerjee, U.C., Synthesis of metallic nanoparticles using plant extracts, Biotechnology advances, 31, 346-356 (2013).

[12] Ahmed, H., Khattab, T.A., Mashaly, H., El-Halwagy, A., Rehan, M., Plasma activation toward multi-stimuli responsive cotton fabric via in situ development of polyaniline derivatives and silver nanoparticles, Cellulose, 27, 2913-2926 (2020).

[13] Mallikarjuna, K., Narasimha, G., Dillip, G., Praveen, B., Shreedhar, B., Lakshmi, C.S., Reddy, B., Raju, B.D.P., Green synthesis of silver nanoparticles using Ocimum leaf extract and their

characterization, Digest Journal of Nanomaterials and Biostructures, 6, 181-186 (2011).
[14] Song, X., Bayati, P., Gupta, M., Elahinia, M., Haghshenas, M., Fracture of magnesium matrix nanocomposites-a review, International Journal of Lightweight Materials and Manufacture, 4, 67-98 (2021).
[15] El-Sheshtawy, H.S., Sofy, M.R., Ghareeb, D.A., Yacout, G.A., Eldemellawy, M.A., Ibrahim, B.M., Eco-friendly polyurethane acrylate (PUA)/natural filler-based composite as an antifouling product for marine coating, Applied Microbiology and Biotechnology, 105, 7023-7034 (2021).
[16] Jyoti, K., Baunthiyal, M., Singh, A., Characterization of silver nanoparticles synthesized using Urtica dioica Linn. leaves and their synergistic effects with antibiotics, Journal of Radiation Research and Applied Sciences, 9, 217-227 (2016).
[17] Emam, H.E., Ahmed, H.B., Abdelhameed, R.M., Melt intercalation technique for synthesis of hetero-metallic@chitin bio-composite as recyclable catalyst for prothiofos hydrolysis, Carbohydrate Polymers, 266, 118163 (2021).
[18] Emam, H.E., Attia, M.A., El-Dars, F.M., Ahmed, H.B., Emerging use of homogenic and heterogenic nano-colloids synthesized via size-controllable technique in catalytic potency, Journal of Polymers and the Environment, 28, 553-565 (2020).
[19] Jogee, S., Ingle, A., Gupta, I., Bonde, S., Rai, M., Detection and management of mycotoxigenic fungi in nuts and dry fruits, in: I International Symposium on Mycotoxins in Nuts and Dried Fruits 963, pp. 69-77 2011.
[20] Ahmed, H.B., Emam, H.E., Seeded growth core-shell (Ag–Au–Pd) ternary nanostructure at room temperature for potential water treatment, Polymer Testing, 89, 106720 (2020).
[21] Panáček, A., Kvitek, L., Prucek, R., Kolář, M., Večeřová, R., Pizúrová, N., Sharma, V.K., Nevěčná, T.j., Zbořil, R., Silver colloid nanoparticles: synthesis, characterization, and their antibacterial activity, The Journal of Physical Chemistry B, 110, 16248-16253 (2006).
[22] Morones, J.R., Elechiguerra, J.L., Camacho, A., Holt, K., Kouri, J.B., Ramírez, J.T., Yacaman, M.J., The bactericidal effect of silver nanoparticles, Nanotechnology, 16, 2346 (2005).
[23] Singh, P., Mijakovic, I., Antibacterial Effect of Silver Nanoparticles Is Stronger If the Production Host and the Targeted Pathogen Are Closely Related, Biomedicines, 10, 628 (2022).
[24] Ahmed, H.B., Mikhail, M.M., El-Sherbiny, S., Nagy, K.S., Emam, H.E., pH responsive intelligent nano-engineer of nanostructures applicable for discoloration of reactive dyes, Journal of colloid and interface science, 561, 147-161 (2020).
[25] Ahmed, H.B., Attia, M.A., El-Dars, F.M., Emam, H.E., Hydroxyethyl cellulose for spontaneous synthesis of antipathogenic nanostructures:(Ag & Au) nanoparticles versus Ag-Au nano-alloy, International journal of biological macromolecules, 128, 214-229 (2019).
[26] Fayaz, A.M., Balaji, K., Girilal, M., Yadav, R., Kalaichelvan, P.T., Venketesan, R., Biogenic synthesis of silver nanoparticles and their synergistic effect with antibiotics: a study against gram-positive and gram-negative bacteria, Nanomedicine: Nanotechnology, Biology and Medicine, 6, 103-109 (2010).
[27] Burgaz, E., Sezener, M.G., Dikbas, C., Ceylan, A.K., Andac, M., Ciftci, A., Determination of antibacterial properties of silver nanoparticles with aqueous extracts of Brassica oleracea L. var. acephala DC in cotton textiles, Journal of Elementology, 26, (2021).
[28] Emam, H.E., Ahmed, H.B., Comparative study between homo-metallic & hetero-metallic nanostructures based agar in catalytic degradation of dyes, International journal of biological macromolecules, 138, 450-461 (2019).
[29] Emam, H.E., Arabic gum as bio-synthesizer for Ag–Au bimetallic nanocomposite using seed-mediated growth technique and its biological efficacy, Journal of Polymers and the Environment, 27, 210-223 (2019).
[30] Ahmed, H.B., Saad, N., Emam, H.E., Recyclable palladium based nano-catalytic laborer encaged within bio-granules for dye degradation, Surfaces and Interfaces, 25, 101175 (2021).
[31] Goud, K.Y., Reddy, K.K., Khorshed, A., Kumar, V.S., Mishra, R.K., Oraby, M., Ibrahim, A.H., Kim, H., Gobi, K.V., Electrochemical diagnostics of infectious viral diseases: Trends and challenges, Biosensors and Bioelectronics, 180, 113112 (2021).
[32] Pan, X., Zhang, Y., Zhao, Y., Yao, S., Guan, C., Wang, L., Chen, L., Inhibitory activity and mechanism of silver nanoparticles against herpes simplex virus type 1, Archives of Virology, 1-18 (2022).
[33] Kleymann, G., Agents and strategies in development for improved management of herpes simplex virus infection and disease, Expert

opinion on investigational drugs, 14, 135-161 (2005).
[34] Roa-Linares, V.C., Miranda-Brand, Y., Tangarife-Castaño, V., Ochoa, R., García, P.A., Castro, M.Á., Betancur-Galvis, L., San Feliciano, A., Anti-herpetic, anti-dengue and antineoplastic activities of simple and heterocycle-fused derivatives of terpenyl-1, 4-naphthoquinone and 1, 4-anthraquinone, Molecules, 24, 1279 (2019).
[35] Agha, M.S., Abbas, M.A., Sofy, M.R., Haroun, S.A., Mowafy, A.M., Dual inoculation of Bradyrhizobium and Enterobacter alleviates the adverse effect of salinity on Glycine max seedling, Notulae Botanicae Horti Agrobotanici Cluj-Napoca, 49, 12461 (2021).
[36] Bacon, T.H., Levin, M.J., Leary, J.J., Sarisky, R.T., Sutton, D., Herpes simplex virus resistance to acyclovir and penciclovir after two decades of antiviral therapy, Clinical microbiology reviews, 16, 114-128 (2003).
[37] Egan, K.P., Wu, S., Wigdahl, B., Jennings, S.R., Immunological control of herpes simplex virus infections, Journal of neurovirology, 19, 328-345 (2013).
[38] Pan, D., Kaye, S.B., Hopkins, M., Kirwan, R., Hart, I.J., Coen, D.M., Common and new acyclovir resistant herpes simplex virus-1 mutants causing bilateral recurrent herpetic keratitis in an immunocompetent patient, The Journal of infectious diseases, 209, 345-349 (2014).
[39] De Paor, M., O'Brien, K., Fahey, T., Smith, S.M., Antiviral agents for infectious mononucleosis (glandular fever), Cochrane Database of Systematic Reviews, (2016).
[40] Maduray, K., Parboosing, R., Metal nanoparticles: a promising treatment for viral and arboviral infections, Biological Trace Element Research, 199, 3159-3176 (2021).
[41] Sethi, P., Activity of turbinaria ornata (Turner) J. Agade against Blue Tongue Virus (Btv), IOSR J Pharm, 6, 93-95 (2016).
[42] Andrighetti-Fröhner, C., Antonio, R., Creczynski-Pasa, T., Barardi, C., Simões, C., Cytotoxicity and potential antiviral evaluation of violacein produced by Chromobacterium violaceum, Memórias do Instituto Oswaldo Cruz, 98, 843-848 (2003).
[43] Wayne, P., National Committee for clinical laboratory standards (NCCLS), methods for dilution antimicrobial susceptibility tests for bacterial that grow aerobically, 6thedn, Approved standard M7-A6, (2003).
[44] Jeevanandam, J., Kiew, S.F., Boakye-Ansah, S., Lau, S.Y., Barhoum, A., Danquah, M.K., Rodrigues, J., Green approaches for the synthesis of metal and metal oxide nanoparticles using microbial and plant extracts, Nanoscale, 14, 2534-2571 (2022).
[45] Matussin, S., Harunsani, M.H., Tan, A.L., Khan, M.M., Plant-extract-mediated SnO2 nanoparticles: synthesis and applications, ACS Sustainable Chemistry & Engineering, 8, 3040-3054 (2020).
[46] Duan, H., Wang, D., Li, Y., Green chemistry for nanoparticle synthesis, Chemical Society Reviews, 44, 5778-5792 (2015).
[47] Avilala, J., Golla, N., Antibacterial and antiviral properties of silver nanoparticles synthesized by marine actinomycetes, Int. J. Pharm. Sci. Res, 10, 1223-1228 (2019).
[48] Abu-Shahba, M.S., Mansour, M.M., Mohamed, H.I., Sofy, M.R., Effect of biosorptive removal of cadmium ions from hydroponic solution containing indigenous garlic peel and mercerized garlic peel on lettuce productivity, Scientia Horticulturae, 293, 110727 (2022).
[49] Amooaghaie, R., Saeri, M.R., Azizi, M., Synthesis, characterization and biocompatibility of silver nanoparticles synthesized from Nigella sativa leaf extract in comparison with chemical silver nanoparticles, Ecotoxicology and Environmental Safety, 120, 400-408 (2015).
[50] Thirunavoukkarasu, M., Balaji, U., Behera, S., Panda, P., Mishra, B., Biosynthesis of silver nanoparticle from leaf extract of Desmodium gangeticum (L.) DC. and its biomedical potential, Spectrochimica Acta Part A: Molecular and Biomolecular Spectroscopy, 116, 424-427 (2013).
[51] Munazza, F., Sadaf Zaidi, N.-u.-S., Amraiz, D., Afzal, F., In vitro antiviral activity of Cinnamomum cassia and its nanoparticles against H7N3 influenza a virus, Journal of Microbiology and Biotechnology, 26, 151-159 (2016).
[52] Kwon, H.-J., Kim, H.-H., Yoon, S.Y., Ryu, Y.B., Chang, J.S., Cho, K.-O., Rho, M.-C., Park, S.-J., Lee, W.S., In vitro inhibitory activity of Alpinia katsumadai extracts against influenza virus infection and hemagglutination, Virology journal, 7, 1-9 (2010).
[53] Ko, H.-C., Wei, B.-L., Chiou, W.-F., The effect of medicinal plants used in Chinese folk medicine on RANTES secretion by virus-infected human epithelial cells, Journal of ethnopharmacology, 107, 205-210 (2006).
[54] Galdiero, S., Falanga, A., Vitiello, M., Cantisani, M., Marra, V., Galdiero, M., Silver nanoparticles as potential antiviral agents, Molecules, 16, 8894-8918 (2011).

[55] Sofy, M.R., Mancy, A.G., Alnaggar, A.E.A.M., Refaey, E.E., Mohamed, H.I., Elnosary, M.E., Sofy, A.R., A polishing the harmful effects of Broad Bean Mottle Virus infecting broad bean plants by enhancing the immunity using different potassium concentrations, Notulae Botanicae Horti Agrobotanici Cluj-Napoca, 50, 12654 (2022).

[56] Morris, D., Ansar, M., Speshock, J., Ivanciuc, T., Qu, Y., Casola, A., Garofalo, R.P., Antiviral and immunomodulatory activity of silver nanoparticles in experimental RSV infection, Viruses, 11, 732 (2019).

[57] Badawy, I.H., Hmed, A.A., Sofy, M.R., Al-Mokadem, A.Z., Alleviation of Cadmium and Nickel Toxicity and Phyto-Stimulation of Tomato Plant L. by Endophytic Micrococcus luteus and Enterobacter cloacae, Plants, 11, 2018 (2022).

[58] Chen, X., Schluesener, H.J., Nanosilver: a nanoproduct in medical application, Toxicology letters, 176, 1-12 (2008).

[59] Matsumura, Y., Yoshikata, K., Kunisaki, S.-i., Tsuchido, T., Mode of bactericidal action of silver zeolite and its comparison with that of silver nitrate, Applied and environmental microbiology, 69, 4278-4281 (2003).

[60] Doty, R.C., Tshikhudo, T.R., Brust, M., Fernig, D.G., Extremely stable water-soluble Ag nanoparticles, Chemistry of Materials, 17, 4630-4635 (2005).

[61] ALHaithloul, H.A.S., Khan, M.I., Musa, A., Ghoneim, M.M., ALrashidi, A.A., Khan, I., Azab, E., Gobouri, A.A., Sofy, M.R., El-Sherbiny, M., Phytotoxic effects of Acacia saligna dry leachates on germination, seedling growth, photosynthetic performance, and gene expression of economically important crops, PeerJ, 10, e13623 (2022).

[62] El-Shennawy, G., Abd Ellatif, R., Badran, S., El-Sokkary, R., Silver nanoparticles: A potential antibacterial and antibiofilm agent against biofilm forming multidrug resistant bacteria, Microbes and Infectious Diseases, 1, 77-85 (2020).

[63] Prabhu, S., Poulose, E.K., Silver nanoparticles: mechanism of antimicrobial action, synthesis, medical applications, and toxicity effects, International nano letters, 2, 1-10 (2012).

[64] Dawood, M.F., Sofy, M.R., Mohamed, H.I., Sofy, A.R., Abdel-kader, H.A., Hydrogen Sulfide Modulates Salinity Stress in Common Bean Plants by Maintaining Osmolytes and Regulating Nitric Oxide Levels and Antioxidant Enzyme Expression, Journal of Soil Science and Plant Nutrition, 1-19 (2022).

[65] Mohamed, H.I., Abd-Elsalam, K.A., Tmam, A.M., Sofy, M.R., Silver-based nanomaterials for plant diseases management: Today and future perspectives, in: Silver Nanomaterials for Agri-Food Applications, Elsevier, 2021, pp. 495-526.

[66] Huang, S., Liu, M., Li, H., In situ green synthesis of lysozyme/silver nanoparticles sol and their antimicrobial properties, New Journal of Chemistry, 46, 11759-11773 (2022).

[67] Musimun, C., Papiernik, D., Permpoonpattana, P., Chumkaew, P., Srisawat, T., Synergy of green-synthesized silver nanoparticles and Vatica diospyroides fruit extract in inhibiting Gram-positive bacteria by inducing membrane and intracellular disruption, Journal of Experimental Nanoscience, 17, 420-438 (2022).

[68] El-Sheshtawy, H.S., Mahdy, H.M., Sofy, A.R., Sofy, M.R., Production of biosurfactant by Bacillus megaterium and its correlation with lipid peroxidation of Lactuca sativa, Egyptian Journal of Petroleum, 31, 1-6 (2022).

[69] Garibo, D., Borbón-Nuñez, H.A., de León, J.N.D., García Mendoza, E., Estrada, I., Toledano-Magaña, Y., Tiznado, H., Ovalle-Marroquin, M., Soto-Ramos, A.G., Blanco, A., Green synthesis of silver nanoparticles using Lysiloma acapulcensis exhibit high-antimicrobial activity, Scientific reports, 10, 1-11 (2020).

[70] Loo, Y.Y., Rukayadi, Y., Nor-Khaizura, M.-A.-R., Kuan, C.H., Chieng, B.W., Nishibuchi, M., Radu, S., In vitro antimicrobial activity of green synthesized silver nanoparticles against selected gram-negative foodborne pathogens, Frontiers in microbiology, 9, 1555 (2018).

[71] Lima, A.K.O., Vasconcelos, A.A., Sousa Júnior, J., Escher, S.K.S., Nakazato, G., Taube Júnior, P., Green Synthesis of Silver Nanoparticles Using Amazon Fruits, International Journal of Nanoscience and Nanotechnology, 15, 179-188 (2019).

[72] Alsamhary, K.I., Eco-friendly synthesis of silver nanoparticles by Bacillus subtilis and their antibacterial activity, Saudi Journal of Biological Sciences, 27, 2185-2191 (2020).

[73] Parvekar, P., Palaskar, J., Metgud, S., Maria, R., Dutta, S., The minimum inhibitory concentration (MIC) and minimum bactericidal concentration (MBC) of silver nanoparticles against Staphylococcus aureus, Biomaterial investigations in dentistry, 7, 105-109 (2020).

[74] Dawood, M.F., Abu-Elsaoud, A.M., Sofy, M.R., Mohamed, H.I., Soliman, M.H., Appraisal of kinetin spraying strategy to alleviate the harmful effects of UVC stress on tomato plants,

Environmental Science and Pollution Research, 1-21 (2022).
[75] Quinteros, M.A., Aiassa Martínez, I.M., Dalmasso, P.R., Páez, P.L., Silver nanoparticles: biosynthesis using an ATCC reference strain of Pseudomonas aeruginosa and activity as broad spectrum clinical antibacterial agents, International journal of biomaterials, 2016, (2016).
[76] Khalil, M.A., El Maghraby, G.M., Sonbol, F.I., Allam, N.G., Ateya, P.S., Ali, S.S., Enhanced efficacy of some antibiotics in presence of silver nanoparticles against multidrug resistant Pseudomonas aeruginosa recovered from burn wound infections, Frontiers in microbiology, 12, (2021).
[77] Hosny, A.E.-D.M., Rasmy, S.A., Aboul-Magd, D.S., Kashef, M.T., El-Bazza, Z.E., The increasing threat of silver-resistance in clinical isolates from wounds and burns, Infection and drug resistance, 12, 1985 (2019).
[78] Tang, S., Zheng, J., Antibacterial activity of silver nanoparticles: structural effects, Advanced healthcare materials, 7, 1701503 (2018).
[79] Saratale, G.D., Saratale, R.G., Benelli, G., Kumar, G., Pugazhendhi, A., Kim, D.-S., Shin, H.-S., Anti-diabetic potential of silver nanoparticles synthesized with Argyreia nervosa leaf extract high synergistic antibacterial activity with standard antibiotics against foodborne bacteria, Journal of Cluster Science, 28, 1709-1727 (2017).
[80] Long, Y.-M., Hu, L.-G., Yan, X.-T., Zhao, X.-C., Zhou, Q.-F., Cai, Y., Jiang, G.-B., Surface ligand controls silver ion release of nanosilver and its antibacterial activity against Escherichia coli, International journal of nanomedicine, 12, 3193 (2017).
[81] Ahluwalia, V., Kumar, J., Sisodia, R., Shakil, N.A., Walia, S., Green synthesis of silver nanoparticles by Trichoderma harzianum and their bio-efficacy evaluation against Staphylococcus aureus and Klebsiella pneumonia, Industrial Crops and Products, 55, 202-206 (2014).